Title

Protoglobin-Catalyzed Formation of cis-Trifluoromethyl-Substituted Cyclopropanes by Carbene Transfer.

Journal

Angewandte Chemie, 62(4)

Authors

Schaus, Lucas
Das, Anuvab
Knight, Anders
et al.

Publication Date

2023-01-23

DOI

10.1002/anie.202208936

Peer reviewed

HHS Public Access

Author manuscript

Angew Chem Int Ed Engl. Author manuscript; available in PMC 2024 January 23.

Published in final edited form as:

Angew Chem Int Ed Engl. 2023 January 23; 62(4): e202208936. doi:10.1002/anie.202208936.

Protoglobin-Catalyzed Formation of *cis*-Trifluoromethyl-Substituted Cyclopropanes by Carbene Transfer

Lucas Schaus[†,[a]], **Anuvab Das**[†,[a]], **Anders M. Knight**[[a]], **Gonzalo Jimenez-Osés**[[b],[c]], **K. N. Houk**[[d]], **Marc Garcia-Borràs**[[e]], **Frances H. Arnold**[[a]], **Xiongyi Huang**[[f]]

[a]Division of Chemistry and Chemical Engineering, California Institute of Technology, 1200 E California Blvd., Pasadena, CA-91125, United States

[b]Center for Cooperative Research in Biosciences (CIC bioGUNE), Basque Research and Technology Alliance (BRTA), Bizkaia Technology Park, Building 800, 48160 Derio, Spain

[c]Ikerbasque, Basque Foundation for Science, 48013 Bilbao, Spain.

[d]Department of Chemistry and Biochemistry, University of California, Los Angeles, CA-90095, United States

[e]Institut de Química Computacional i Catàlisi and Departament de Química, Universitat de Girona, C/ M. Aurèlia Capmany, 69, 17003 Girona, Spain

[f]Department of Chemistry, Johns-Hopkins University, Baltimore, MD-21218, United States

Abstract

Trifluoromethyl-substituted cyclopropanes (CF_3-CPAs) constitute an important class of compounds for drug discovery. While several methods have been developed for synthesis of *trans*-CF_3-CPAs, stereoselective production of corresponding *cis*-diastereomers remains a formidable challenge. We report a biocatalyst for diastereo- and enantio-selective synthesis of *cis*-CF_3-CPAs with activity on a variety of alkenes. We found that an engineered protoglobin from *Aeropyrnum pernix* (*Ape*Pgb) can catalyze this unusual reaction at preparative scale with low-to-excellent yield (6–55%) and enantioselectivity (17–99% ee). Computational studies revealed that the steric environment in the active site of the protoglobin forced iron-carbenoid and substrates to adopt a pro-*cis* near-attack conformation. This work demonstrates the capability of enzyme catalysts to tackle challenging chemistry problems and provides a powerful means to expand the structural diversity of CF_3-CPAs for drug discovery.

Graphical Abstract

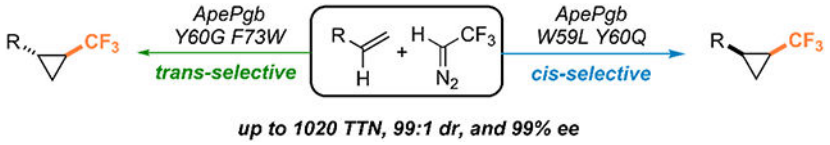

frances@cheme.caltech.edu; marc.garcia@udg.edu; xiongyi@jhu.edu, Twitter username: @xiongyih (for X.H.); @MarcGBQ (for M.G.B.); @francesarnold (For F.H.A).

†These authors contributed equally to this work

Protoglobins were engineered to catalyze stereodivergent cyclopropanation to afford a variety of trifluoromethyl-substituted cyclopropanes using trifluorodiazoethane as the trifluoromethyl-carbene precursor.

Keywords

Biocatalysis; Cyclopropanes; Organofluorines; Protoglobins; Carbenes

Fluorine-containing molecules (organofluorines) have become one of the most important classes of compounds in medicinal chemistry, with recent reports stating that 20% of the marketed drugs contain fluorine.[1-2] Among various organofluorines for pharmaceutical development, trifluoromethyl-substituted cyclopropanes (CF_3-CPAs) have assumed a privileged position, as they combine the conformational rigidity of cyclopropanes and desirable medicinal properties of trifluoromethyl groups in one moiety.[3-4] Furthermore, CF_3-CPAs are widely used as bioisosteres to replace labile *tert*-butyl groups in drug leads to improve their bioavailability and metabolic stability, making them highly valuable for the pharmaceutical industry.[4]

Because of the prevalence of CF_3-CPAs in medicinal chemistry, there are continuous efforts in developing catalytic methods for enantioselective synthesis of CF_3-CPAs (Scheme 1).[5-7] Despite considerable progress, a few challenges remain. One is the limited substrate scope, as most methods developed so far have focused on cyclopropanation of styrenes and arene-substituted alkenes.[4-6, 8-14] Furthermore, the majority of current catalytic methods only produced the *trans*-diastereomer of CF_3-CPAs, which is often thermodynamically and kinetically favored.[7, 15-17] Accessing *cis*-CF_3-CPAs is considerably harder, most likely due to an additional steric challenge posed in the pro-*cis* transition state.[7] The only method reported to selectively synthesize *cis*-CF_3-CPA used a Corey-Chaykovski reaction on highly electron-deficient β-nitrostyrenes;[10] it is neither catalytic nor enantioselective. Gaining access to *cis*-trifluoromethyl-substituted cyclopropanes will be valuable for full exploitation of CF_3-CPAs for drug development, as it is known that molecular topologies of *cis*- and *trans*-cyclopropanes are quite different and often lead to drastic differences in their biological properties.[18]

In this work, we present a method to synthesize *cis*-trifluoromethyl-substituted cyclopropanes using new laboratory-evolved variants of *Aeropyrnum pernix* and *Methanosarcina acetivorans* protoglobins (denoted as *Ape*Pgb and *Ma*Pgb, respectively). Previous work from this laboratory showed that *Ape*Pgb could be engineered to catalyze the cyclopropanation of unactivated alkenes using ethyl diazoacetate, yielding corresponding *cis*-cyclopropanes.[19] Thus, we speculated that protoglobins can be evolved to catalyze the challenging synthesis of *cis*-CF_3-CPAs despite the fact that iron-porphyrin catalysts overwhelmingly produce the *trans* products.[11, 20]

Driven by this hypothesis, we screened several of the previously engineered protoglobin catalysts for initial activity for production of *cis*-CF_3-CPAs. For screening conditions, we prepared solutions of trifluorodiazoethane via a protocol first reported by Gilman *et al.* (SI Experimental 2).[21] This approach has been demonstrated to enable sufficiently high

screening throughput during both initial activity search and consecutive enzyme engineering steps.[22] Through this initial screening, we found that wild-type *Ape*Pgb can catalyze the formation of *cis*-CF_3-CPA **1** with a total turnover number (TTN) of 110 (SI table 1).

We next carried out site-saturation mutagenesis (SSM) and screening on four sites including W59, Y60, F73, and F145. These four sites were chosen based on their proximity to the heme center. Previous studies also showed that they were important for regulating the stereoselectivity of carbene-transfer reactions catalyzed by *Ape*Pgb.[19] Through this engineering, we were able to improve the TTN of *Ape*Pgb for this abiological reaction to 420 (3.8-fold improvement) by introducing two mutations, W59L and Y60Q. This is the first example of a catalytic method that can selectively produce *cis*-CF_3-CPAs from alkenes. The *Ape*Pgb W59L Y60Q (*Ape*Pgb LQ) variant showed activity on a broad range of olefins including electron-rich and electron-deficient styrenes, unactivated alkenes, and heteroatom-substituted alkenes. The diastereo- and enantioselectivities were moderate to excellent for most tested substrates (Figure 1a). The yields ranged from 6% to 55% in a 1-mmol-scale reaction using lyophilized powder of whole *Escherichia coli* cells expressing the *Ape*Pgb LQ variant. Products **1**, **2,** and **3** were particularly interesting since neither the *cis* nor the *trans* forms of these compounds have been synthesized previously. And the successful production of **2** and **3** showed that this method could be used to synthesize quaternary chiral centers.

During the evolution of the *Ape*Pgb LQ variant, we learned that mutations at position F73 can dramatically influence the diastereoselectivity of *Ape*Pgb catalysts. We performed further rounds of SSM at residues W59, Y60, and F73, resulting in the discovery of an *Ape*Pgb Y60G F73W (GW) variant which selectively catalyzed the formation of the *trans* product for the benzyl acrylate model substrate (Figure 1b). To further expand the synthetic utility of this catalytic system, we tested whether the key LQ and GW mutations identified for *Ape*Pgb could be transferred to the protoglobin from *Methanosarcina acetivorans* (*Ma*Pgb, 57% sequence identity to *Ape*Pgb). In all cases, *Ma*Pgb LQ and *Ma*Pgb GW achieved the diastereoselectivity observed with the *Ape*Pgb variants. One exception was benzyl methacrylate substrate, with which the *Ma*Pgb GW variant showed notably reduced preference for generating product **2** compared to its *Ape*Pgb counterpart (SI Table 1). These results demonstrate the utility of protoglobins for stereoselective synthesis of CF_3-CPAs.

Next, we explored the origins of the divergent selectivity observed in these engineered protoglobins. Because of the high structural and sequence similarity between *Ma*Pgb (PDB: 2VEB)[23-25] and *Ape*Pgb,[26] we based our *in-silico* studies on *Ma*Pgb variants since there were more structural data available for *Ma*Pgb. We first performed density functional theory (DFT) calculations on a truncated computational model to evaluate the intrinsic reactivity of histidine-ligated iron-heme for CF_3-cyclopropanation in a protein-free environment (see SI for details). Our results revealed that a radical stepwise mechanism was likely, due to the presence of the strong electron-withdrawing CF_3 group on the iron-carbene intermediate and the electron-deficient character of the alkene substrates (SI Figures 2-4), which was consistent with previous computational studies on truncated models of related heme-protein carbene systems.[27] Our transition-state analysis revealed that formation of the first C–C bond in the cyclopropane ring (TS1) was intrinsically favored for generating the *trans*-diastereomer over the *cis*-isomer for both benzyl acrylate ($\Delta\Delta G^{\ddagger}$ =

2.6 kcal·mol^{-1}) and benzyl methacrylate ($\Delta\Delta G^{\ddagger}$ = 2.0 kcal·mol^{-1}) substrates (SI Figures 3 and 5). These calculations were in line with previous experimental studies which showed that iron-porphyrin catalysts overwhelmingly produced *trans* products for cyclopropanation.[11, 20] These results were also consistent with previous computational studies in which *trans*-cyclopropanation was found to be the lowest-energy pathway and was preferred over the *cis*-cycloproanation pathway by about 1.7 kcal·mol^{-1}.[15-16] Our computational data also indicated that after generation of the radical intermediate after the first C—C bond formation, no stereo-scrambling is likely to occur prior to a fast second C–C bond formation step to generate the cyclopropane ring (SI Figure 2).[27] Overall, these results suggested that, for cyclopropanation mediated by a histidine-ligated heme-carbene complex in free solution, the formation of *trans*-CF_3-CPA products would be intrinsically favored. Therefore, the active-site environment of the proteins must play a crucial role in overcoming this intrinsic barrier and redirecting the reaction to selectively form *cis*-CF_3-CPAs.

To further investigate this, we first modelled the iron-carbene intermediate in the active sites of wild-type *Ma*Pgb and the *Ma*Pgb LQ and GW variants using molecular dynamics (MD) simulations (Figure 2, see SI for details), as we have done previously for similar systems.[28-31] MD simulations showed that the iron-carbenoid explored two major conformations in the *Ma*Pgb active sites, whose geometric features were influenced directly by the mutations introduced. In wild-type *Ma*Pgb and *Ma*Pgb LQ, which are *cis*-selective, the iron-carbenoids mainly explore orientations with a ∠N-Fe-C-C(CF_3) dihedral angle around −25° and +50°, respectively, whereas the preferred conformer for the carbenoid in the *trans*-selective *Ma*Pgb GW variant is described by a ∠N-Fe-C-C(CF_3) angle of around −100° and −140° (Figure 2A-B, and SI Figure 6). Under these iron-carbenoid conformations, assuming a similar binding pose for the substrate in the active site of different protoglobin variants (SI Figure 8), wild-type *Ma*Pgb and variant *Ma*Pgb LQ would preferentially lead to the *cis*-diastereomer and variant *Ma*Pgb GW would mainly afford the *trans*-diastereomer. These results suggest that the introduced mutations change the geometric constraints in the active site and switch iron-carbenoid orientation, which ultimately controlled the diastereoselectivity of the reaction (Figure 2C-D, and SI Figures 7-8).

Under this mechanistic scheme, however, there is one exception. *Ma*Pgb GW preferentially produces the *cis* diastereomer in the reaction with benzyl methacrylate (SI Table S1). To further explore the origins of opposite selectivities offered by *Ma*Pgb LQ and GW variants, we performed restrained MD simulations with both substrates bound in LQ and GW active sites. Starting from structures corresponding to the preferred carbenoid-bound major conformers in LQ and GW *Ma*Pgb variants, benzyl acrylate (**11**) and benzyl methacrylate (**12**) were docked into the active site. These structures were then used to start 500-ns MD trajectories in which the substrates were restrained at distances between 2.5–3.5 Å from the iron-carbenoid in order to analyze accessible near-attack conformations (NAC) that they could explore with respect to the iron-carbenoid and to avoid exploring unbinding events (see SI for details).[28] To study the relative orientations of the alkene and iron-carbenoid, geometric parameters based on two dihedral angles were defined which allowed us to characterize the pro-*cis*/*trans* character of the NACs explored by the substrate and the carbene in each variant-substrate pair along the MD trajectories (Figure 3, relative

orientation of the alkene is defined by the orange dihedral angle, and the relative orientation of the iron-carbenoid by the blue dihedral angle).

These simulations revealed that when both substrates (benzyl acrylate **11** and benzyl methacrylate **12** in Figure 3) were bound in the *Ma*Pgb LQ active site, they mainly explored a major near-attack conformation with respect to the carbenoid, which corresponded to a *cis*-selective configuration (Figures 3A-B and SI Figure 9, dihedral values ca. +130° (alkene, in orange) and −90° (carbenoid, in blue)). This was due to the preorganization of the iron-carbenoid intermediate in the active site and the steric requirements applied to the substrate when placed in the binding pocket in a catalytically competent pose. In contrast, *Ma*Pgb GW preferentially bound the benzyl acrylate substrate in a slightly different catalytic pose to that in the LQ variant, whereas the iron-carbenoid was rotated, as previously observed in carbene-bound simulations (Figures 3A-B and SI Figure 9, dihedral values ca. +130° (alkene, in orange) and +90° (carbenoid, in blue)). This alternative near-attack conformation led to the preferential formation of the *trans*-diastereomer, in line with the experimentally observed selectivity switch. Consequently, we propose that different orientations explored by the iron-carbenoid in the active sites of the LQ and GW *Ma*Pgb variants are responsible for controlling the selectivity of these reactions and overcoming the intrinsic electronic preferences to yield almost exclusively the *cis*-diastereomer.

Finally, simulations with the benzyl methacrylate substrate bound in the *Ma*Pgb GW variant described a preferential near-attack conformation that led to the *cis*-cyclopropane product (Figures 3A-B and SI Figure 9, dihedral values ca. +130° (alkene, in orange) and −90° (carbenoid, in blue)). These simulations showed that due to the extra steric bulk of the methyl group at the alkene α-position and the *Ma*Pgb GW active-site environment, the iron-carbenoid was forced to rotate when the olefin approaches, as compared to the benzyl acrylate system. Consequently, the iron-carbenoid and benzyl methacrylate preferentially explored near-attack pro-*cis* conformations due to steric requirements in the GW variant active site. These results illustrate why *Ma*Pgb GW was not able to produce the *trans*-cyclopropane in the case of benzyl methacrylate (SI Scheme 1).

Herein, we report a catalytic and enantioselective method for producing *cis*-trifluoromethyl-substituted cyclopropanes. Additionally, we have shown that the biocatalysts are active on a wide range of substrates, including non-aryl-substituted alkenes and unactivated alkenes. Their *cis*-selectivity is likely controlled by the active-site geometry, which preorganizes the iron-carbenoid and the substrate in a pro-*cis* near-attack conformation to overcome the intrinsic *trans* preference of the reaction. The reactions were performed using lyophilized whole-cell powders, which can be stored easily and used by those without any cell-culture experience. This new catalytic method to make *cis*-trifluoromethyl-substituted cyclopropanes provides a new, green route to their production and has the potential to become a valuable approach for producing new biologically active compounds.

Supplementary Material

Refer to Web version on PubMed Central for supplementary material.

Acknowledgements

The authors thank Dr. Sabine Brinkmann-Chen for critical reading of the manuscript. This research is supported by the NSF Division of Molecular and Cellular Biosciences (2016137); the Spanish Ministry of Science and Innovation MICINN (grant PID2019-111300GA-I00 and RYC2020-028628-I fellowship to M.G.B; and grant RTI2018-099592-B-C22 to G.J.-O.); the National Institute for General Medical Sciences (grant R00GM129419 to X.H.). L.S. is grateful to the Fonds National de la Recherche Luxembourg (FNR) for an AFR individual PhD grant. The content is solely the responsibility of the authors and does not necessarily represent the official views of the NSF. A.M.K. acknowledges support from the NSF Graduate Research Fellowship (Grant No. DGE-1745301).

References

[1]. Inoue M, Sumii Y, Shibata N, ACS Omega 2020, 5, 10633–10640. [PubMed: 32455181]

[2]. Muller K, Faeh C, Diederich F, Science 2007, 317, 1881–1886. [PubMed: 17901324]

[3]. Talele TT, J. Med. Chem 2016, 59, 8712–8756. [PubMed: 27299736]

[4]. Bos M, Poisson T, Pannecoucke X, Charette AB, Jubault P, Chem. Eur. J 2017, 23, 4950–4961. [PubMed: 27813216]

[5]. Morandi B, Mariampillai B, Carreira EM, Angew. Chem. Int. Ed 2011, 50, 1101–1104.

[6]. Tinoco A, Steck V, Tyagi V, Fasan R, J. Am. Chem. Soc 2017, 139, 5293–5296. [PubMed: 28366001]

[7]. Costantini M, Mendoza A, ACS Catal. 2021, 11, 13312–13319. [PubMed: 34765283]

[8]. Duncton MA, Singh R, Org. Lett 2013, 15, 4284–4287. [PubMed: 23952128]

[9]. Mykhailiuk PK, Afonin S, Ulrich AS, Komarov IV, Synthesis 2006, 11, 1757–1759.

[10]. Hock KJ, Hommelsheim R, Mertens L, Ho J, Nguyen TV, Koenigs RM, J. Org. Chem 2017, 82, 8220–8227. [PubMed: 28636362]

[11]. Morandi B, Carreira EM, Angew Chem Int Ed 2010, 49, 938–941.

[12]. Fuchibe K, Oki R, Hatta H, Ichikawa J, Chem. Eur. J 2018, 24, 17932–17935. [PubMed: 30402967]

[13]. Risse J, Fernandez-Zumel MA, Cudre Y, Severin K, Org. Lett 2012, 14, 3060–3063. [PubMed: 22630342]

[14]. Duan Y, Lin JH, Xiao JC, Gu YC, Org. Lett 2016, 18, 2471–2474. [PubMed: 27169696]

[15]. Wei Y, Tinoco A, Steck V, Fasan R, Zhang Y, J. Am. Chem. Soc 2018, 140, 1649–1662. [PubMed: 29268614]

[16]. Tinoco A, Wei Y, Bacik JP, Carminati DM, Moore EJ, Ando N, Zhang Y, Fasan R, ACS Catal. 2019, 9, 1514–1524. [PubMed: 31134138]

[17]. Carminati DM, Decaens J, Couve-Bonnaire S, Jubault P, Fasan R, Angew. Chem. Int. Ed 2021, 60, 7072–7076.

[18]. Kazuta Y, Matsuda A, Shuto S, J. Org. Chem 2002, 67, 1669–1677. [PubMed: 11871901]

[19]. Knight AM, Kan SBJ, Lewis RD, Brandenberg OF, Chen K, Arnold FH, ACS Cent. Sci 2018, 4, 372–377. [PubMed: 29632883]

[20]. Le Maux P, Juillard S, Simonneaux G, Synthesis 2006, 10, 1701–1702.

[21]. Gilman H, Jones RG, J. Am. Chem. Soc 1943, 65, 1458–1460.

[22]. Zhang J, Huang X, Zhang RK, Arnold FH, J. Am. Chem. Soc 2019, 141, 9798–9802. [PubMed: 31187993]

[23]. Pesce A, Tilleman L, Donne J, Aste E, Ascenzi P, Ciaccio C, Coletta M, Moens L, Viappiani C, Dewilde S, Bolognesi M, Nardini M, PLoS One 2013, 8, e66144. [PubMed: 23776624]

[24]. Pesce A, Bolognesi M, Nardini M, Adv. Microb. Physiol 2013, 63, 79–96. [PubMed: 24054795]

[25]. Ciaccio C, Pesce A, Tundo GR, Tilleman L, Bertolacci L, Dewilde S, Moens L, Ascenzi P, Bolognesi M, Nardini M, Coletta M, Biochim. Biophys. Acta 2013, 1834, 1813–1823. [PubMed: 23485914]

[26]. Porter NJ, Danelius E, Gonen T, Arnold FH, J. Am. Chem. Soc 2022, 144, 8892–8896. [PubMed: 35561334]

[27]. Carminati DM, Fasan R, ACS Catal. 2019, 9, 9683–9697. [PubMed: 32257582]

[28]. Garcia-Borràs M, Kan SBJ, Lewis RD, Tang A, Jimenez-Osés G, Arnold FH, Houk KN, J. Am. Chem. Soc 2021, 143, 7114–7123. [PubMed: 33909977]

[29]. Fasan R, Vargas DA, Ren X, Sengupta A, Zhu L, Garcia-Borràs M, Houk K, 2022, Preprint available at Research Square 10.21203/rs.3.rs-1639676/v1.

[30]. Liu Z, Calvó-Tusell C, Zhou AZ, Chen K, Garcia-Borràs M, Arnold FH, Nat. Chem 2021, 13, 1166–1172. [PubMed: 34663919]

[31]. Calvó-Tusell C, Liu Z, Chen K, Arnold FH, Garcia-Borràs M, 2022, Preprint available at ChemRxiv DOI: 10.26434/chemrxiv-2022-f02xh.

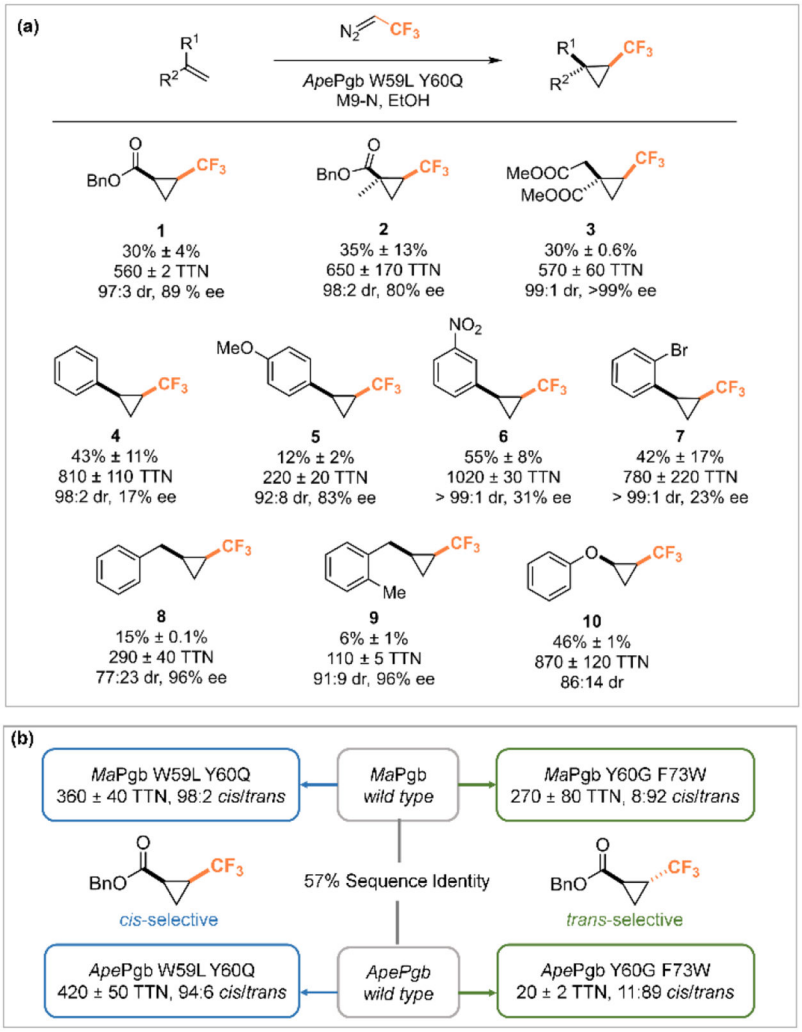

Figure 1.

(a) Substrate scope of the cyclopropanation reaction of trifluorodiazoethane with an alkene, catalyzed by *ApePgb* LQ. Yields, diastereomeric ratios (dr), enantiomeric excess (ee), and TTNs of the reactions are reported. Yields are reported as analytical yields measured via ^{19}F-NMR against 4-fluoroacetophenone of known concentration. Reactions were run at 1-mmol scale with lyophilized whole-cell powder at OD_{600} = 45 in M9-N buffer with 2.5% ethanol as co-solvent. Absolute configurations were not determined. (b) Stereo-divergent cyclopropanation with trifluorodiazoethane catalyzed by engineered protoglobins. Reactions were carried out in small-scale 96-well format, details see SI Table 1.

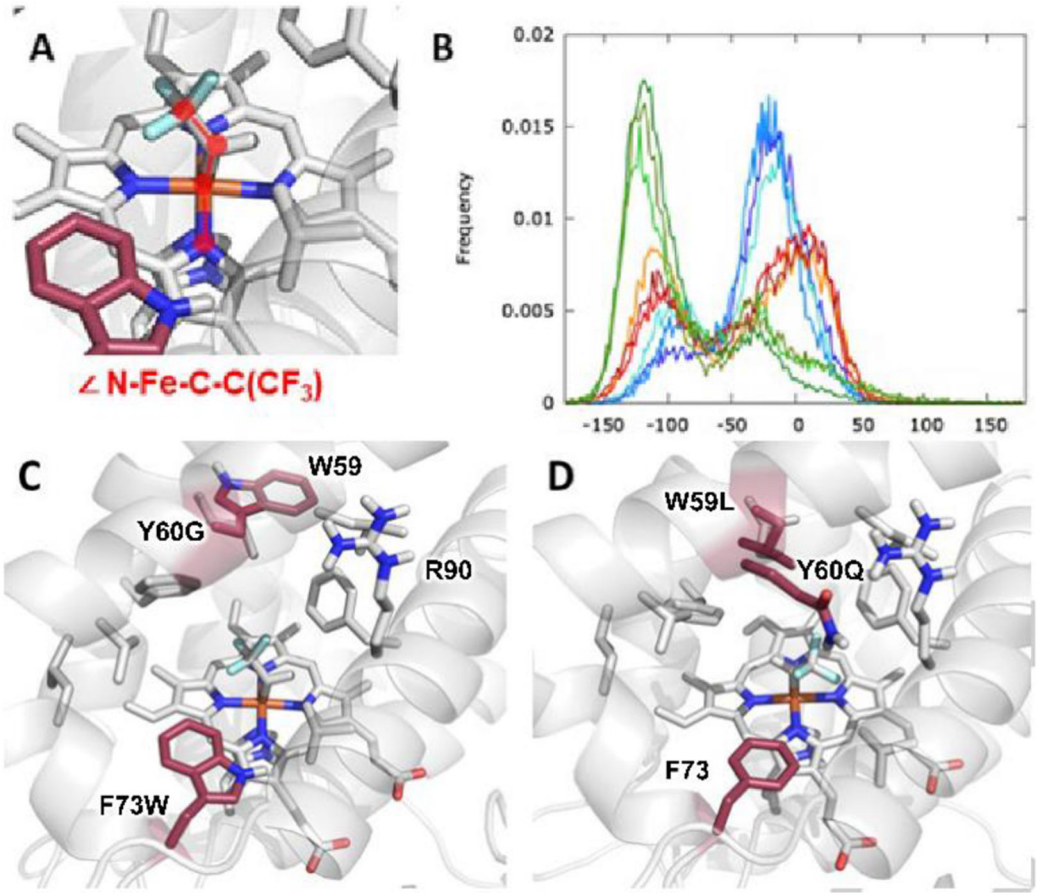

Figure 2.

Computational modelling, based on MD simulations, to characterize the iron-carbenoid formed in the active site of wild-type *Ma*Pgb and *Ma*Pgb LQ and *Ma*Pgb GW variants. A) Active site of *Ma*Pgb GW with the carbenoid bound to heme. The ∠N-Fe-C-C(CF3) dihedral angle measured along the MD trajectories, highlighted in red, describes the relative orientation of the iron-carbene in the active site. B) Histogram describing the dihedral angles explored by the carbenoid relative to heme along MD simulations. Three independent MD replicas of 500 ns each are conducted for each system, shown in three color shades: three red tones for wild-type *Ma*Pgb, three blue tones for *Ma*Pgb LQ, and three green tones for *Ma*Pgb GW (see SI for complete data). Representative snapshots of the major orientation explored in C) *Ma*Pgb GW (∠N-Fe-C-C(CF3) = −117°); and in D) *Ma*Pgb LQ (∠N-Fe-C-C(CF3) = +49°).

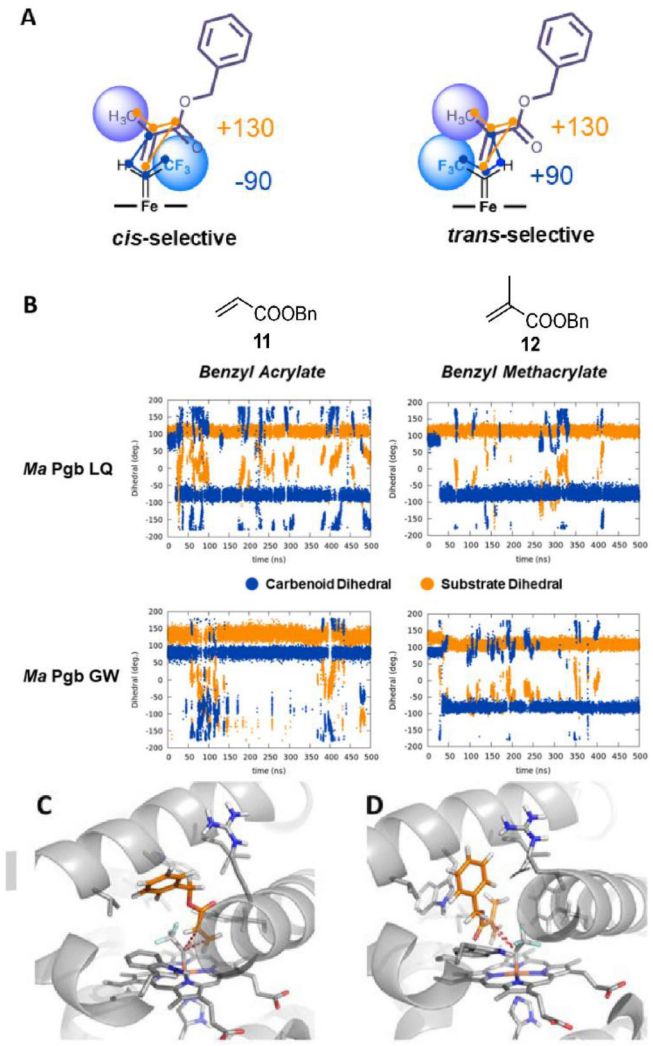

Figure 3.

Computational modelling, based on restrained-MD simulations, to characterize the substrate bound in a catalytically competent pose relative to the iron-carbenoid in variants *Ma*Pgb LQ and GW. (A) Two different dihedral angles were defined to describe the relative orientation of the substituted alkene and the iron-carbenoid along substrate-bound MD simulations. These geometric parameters define which faces of the alkene and the carbenoid are exposed to each other. In orange: ∠C(carbene)-C(alkene)-C(=O)-C(CH_3) dihedral angle describes which face of the alkene is exposed to the carbenoid. In blue: ∠C(alkene)-H(carbene)-C(carbene)-C(CF_3) dihedral angle describes which face of the carbenoid is exposed to the alkene. Different combinations of dihedral angle values describe near attack conformations (NAC) that could produce *cis* or *trans* diastereomers. (B) Dihedral angles measured along 500 ns MD trajectories for *Ma*Pgb LQ/GW variants and benzyl acrylate/methacrylate substrates. Benzyl acrylate bound in *Ma*Pgb LQ mainly explores pro-*cis* NACs, while it mainly explores pro-*trans* NACs in the GW variant. Benzyl methacrylate mainly explores pro-*cis* NACs in both LQ and GW variants. (C) Representative snapshot taken from MD

simulations of *Ma*Pgb GW with benzyl acrylate and (D) of *Ma*Pgb GW with benzyl methacrylate. For similar snapshots in *Ma*Pgb LQ, see SI Figure 9.

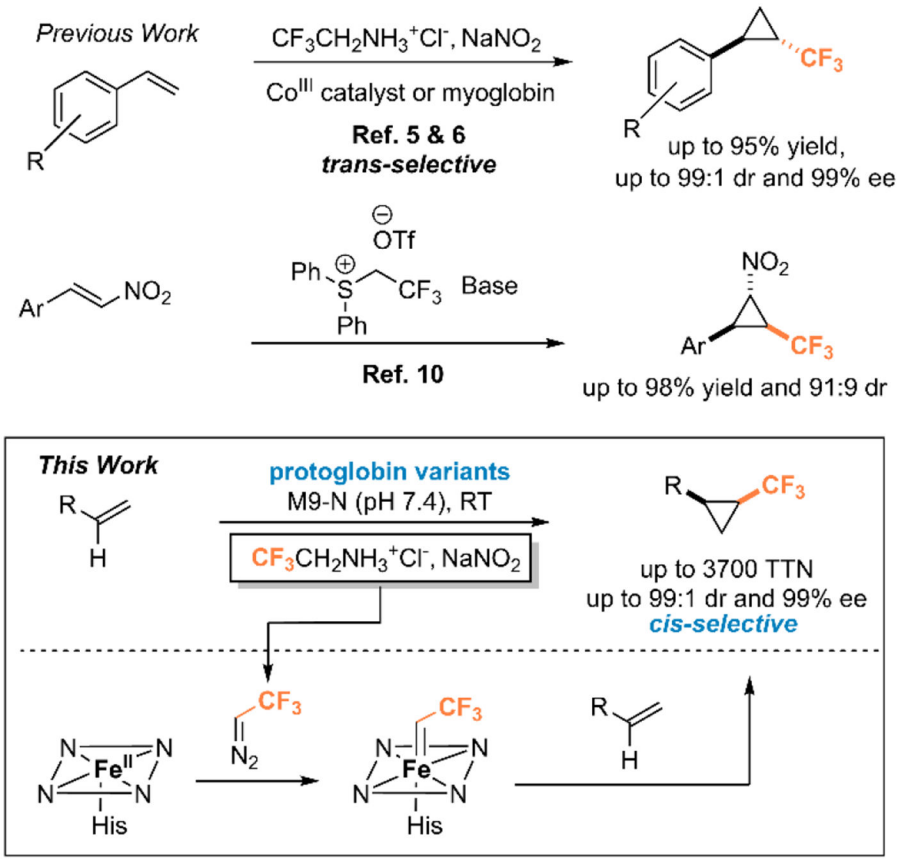

Scheme 1.
Current strategies for synthesis of CF3-CPAs.